iScience

CellPress
OPEN ACCESS

Article

High-frequency neural activity dysregulation is associated with sleep and psychiatric disorders in BMAL1-deficient animal models

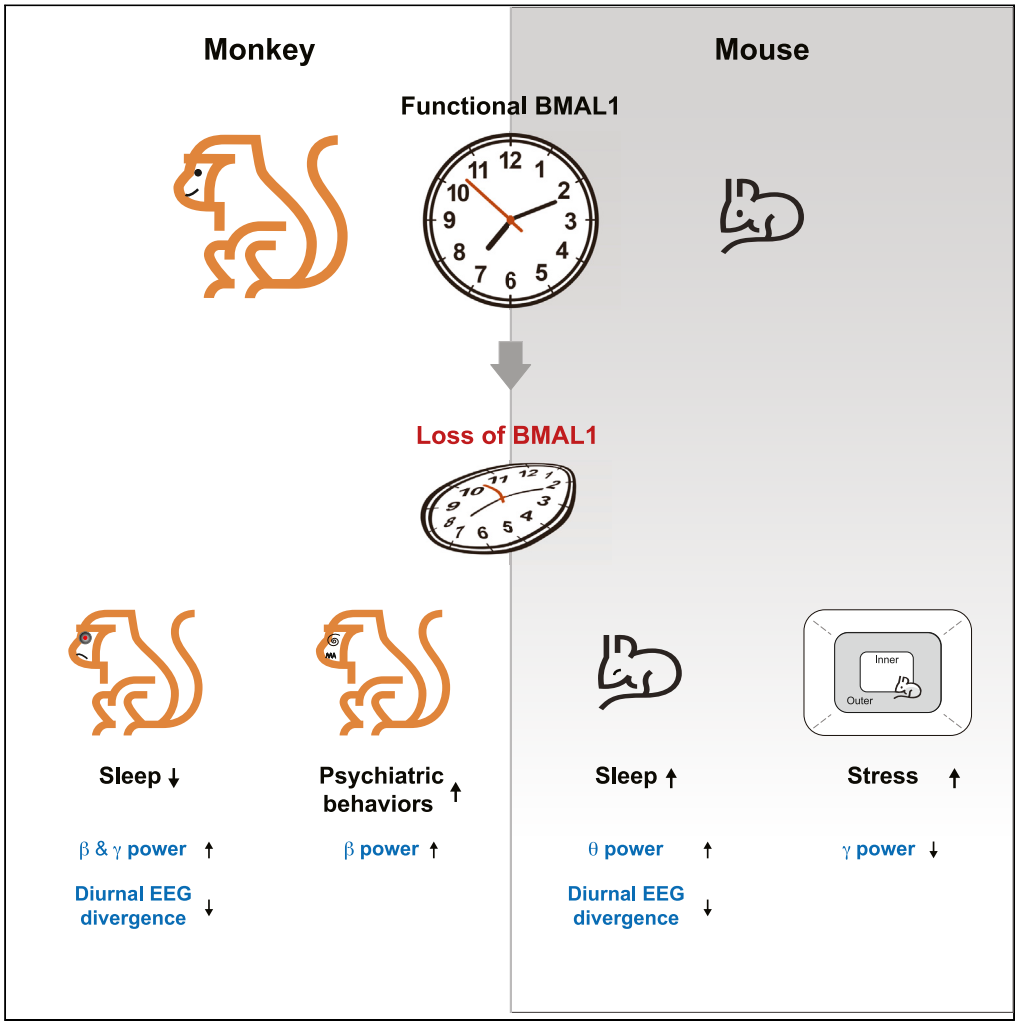

Yu Sun, Mingzhu Zhong, Niannian Xu, ..., Jian Jiang, Yun-Chi Tang, Hung-Chun Chang

hcchang@lglab.ac.cn

Highlights

BMAL1-deficient mice and monkeys exhibit different diurnal EEG power patterns

BMAL1-deficiency leads to dysregulated high-frequency oscillations

Dysregulated β and γ powers mark psychiatric phenotypes in BMAL1-KO monkeys

Sun et al., iScience 27, 109381
April 19, 2024
https://doi.org/10.1016/j.isci.2024.109381

iScience

CellPress
OPEN ACCESS

Article

High-frequency neural activity dysregulation is associated with sleep and psychiatric disorders in BMAL1-deficient animal models

Yu Sun,[1,2,4] Mingzhu Zhong,[1,2,4] Niannian Xu,[1,2,4] Xueting Zhang,[1] Huanhuan Sun,[1] Yan Wang,[2] Yong Lu,[2] Yanhong Nie,[2] Qing Li,[1] Qiang Sun,[2] Jian Jiang,[2] Yun-Chi Tang,[1] and Hung-Chun Chang[1,2,3,5,*]

SUMMARY

Sleep disturbance led by BMAL1-deficiency has been recognized both in rodent and non-human primate models. Yet it remained unclear how their diurnal brain oscillations were affected upon BMAL1 ablation and what caused the discrepancy in the quantity of sleep between the two species. Here, we investigated diurnal electroencephalographs of BMAL1-deficient mice and cynomolgus monkeys at young adult age and uncovered a shared defect of dysregulated high-frequency oscillations by Kullback-Leibler divergence analysis. We found beta and gamma oscillations were significantly disturbed in a day versus night manner in BMAL1-deficient monkeys, while in mice the beta band difference was less evident. Notably, the dysregulation of beta oscillations was particularly associated with psychiatric behaviors in BMAL1-deficient monkeys, including the occurrence of self-injuring and delusion-like actions. As such psychiatric phenotypes were challenging to uncover in rodent models, our results offered a unique method to study the correlation between circadian clock dysregulation and psychiatric disorders.

INTRODUCTION

Disruption of circadian rhythms is known to be associated with multiple diseases, such as cardiovascular dysfunction, diabetic mellitus, cancer, sleep disorders, psychiatric disorders, and neurodegenerative diseases.[1–7] While dysfunctions in peripheral tissues can be investigated at molecular, cellular, and pathological levels in detail for the links with circadian clock disturbance in common animal models then correlate to human symptoms, it was challenging to meet the same resolutions for brain diseases. The difficulty derives from various dissimilarities between common animal models and humans at the structural level, e.g., cell organization and brain structure differences, and functional level, meaning the comparison of cognitive or mental status based on neural imaging or oscillation data. Diurnal-versus nocturnal-active variance adds another layer of complexity when relating circadian clock conditions from human patients to common mammal models such as mice. The mouse model is often imperfect in resembling key brain disease features, particularly the neuropsychiatric symptoms observed in human patients, thus delaying the findings of biomarkers and therapies specific to the symptoms. The joint use of the non-human primate model could offer a solution to such limits. Non-human primates show comparable brain oscillations[8] and sleep patterns[9] with human. Furthermore, non-human primate models display mental disease-related social and cognitive irregularities better than rodent models.[10–12]

To study brain rhythm characteristics associated with circadian clock disturbance and explore potential biomarkers for connecting circadian dysregulation, sleep disorders, and psychiatric diseases, we applied BMAL1-ablated mouse[13] and cynomolgus monkey[14,15] models for the approach. BMAL1 is a crucial component of the CLOCK-BMAL1 transcription factor complex, which activates the expression of a great number of circadian genes. BMAL1-deficient mouse models have been studied for several diseases, such as diabetes,[16] aging,[17] inflammation[18] and sleep disorders.[19] Yet psychiatric disorders,[20] particularly demonstrated by electrophysiological methods remained scarce. In the study, we compared sleep and electroencephalography patterns of BMAL1-deficient mouse and monkey models through standard sleep analysis, spectrogram, and EEG band power assessment. Whilst all methods could indicate dissimilarities between wild-type and BMAL1-deficient models in different manners, we noted Kullback-Leibler divergence[21] is the most convenient test to conclude the change of circadian homeostasis and band power at the same time. Furthermore, as BMAL1-deficient monkeys displayed prominent psychotic phenotypes, we were able to grade irregular behaviors together with brain wave patterns and then proposed EEG biomarkers to respective abnormal

[1]Lingang Laboratory, Shanghai 201203, China
[2]Institute of Neuroscience, State Key Laboratory of Neuroscience, CAS Center for Excellence in Brain Science and Intelligence Technology, University of Chinese Academy of Sciences, Chinese Academy of Sciences, Shanghai 200031, China
[3]Shanghai Center for Brain Science and Brain-Inspired Intelligence Technology, Shanghai 201210, China
[4]These authors contributed equally
[5]Lead contact
*Correspondence: hcchang@lglab.ac.cn
https://doi.org/10.1016/j.isci.2024.109381

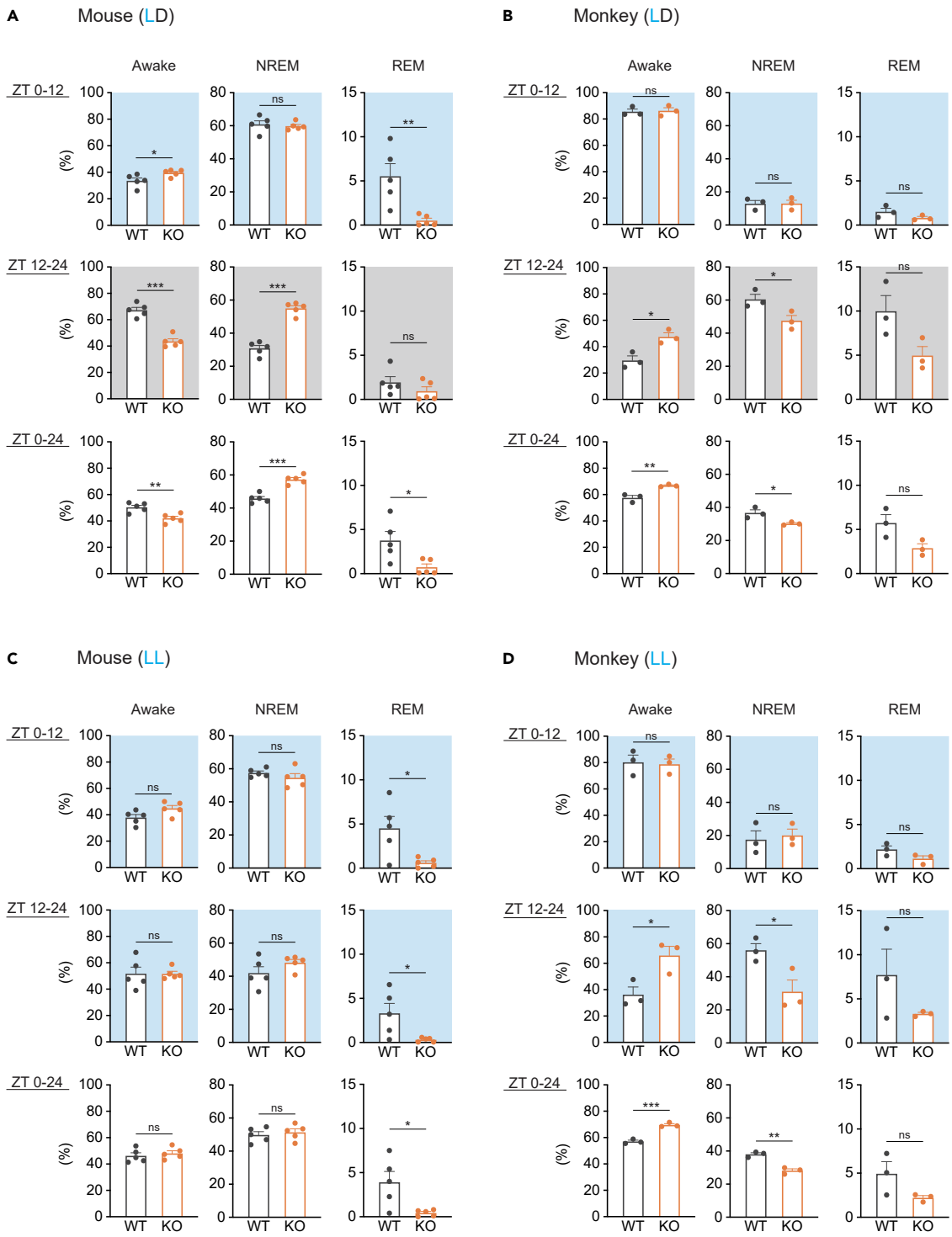

Figure 1. Sleep phenotypes of BMAL1-deficient cynomolgus monkeys and mice

(A) Proportion of awake, NREM sleep and REM sleep during light-on period (7:00-19:00, ZT 0–12), light-off period (19:00-7:00 ZT 12–24) and full day (ZT 0–24) under normal 12 h light-12 h dark (L/D) cycle. 4-month-old wild-type (male n = 2, female n = 3) and Bmal1-KO mice (male n = 2, female n = 3) were applied.

(B) Proportion of awake, NREM sleep and REM sleep during ZT 0–12, ZT 12–24 and full day ZT 0–24 under normal 12 h light-12 h dark (L/D) cycle. 5-year-old wild-type (male n = 2, female n = 1) and BMAL1-KO monkey (male n = 2, female n = 1) were applied.

(C) Proportion of awake, NREM sleep and REM sleep during ZT 0–12, ZT 12–24 and full day ZT 0–24 under constant illumination (L/L) cycle. Same mouse cohort as in (A) were shown.

Figure 1. *Continued*

(D) Proportion of awake, NREM sleep and REM sleep during ZT 0–12, ZT 12–24 and full day ZT 0–24 under constant illumination (L/L) cycle. Same monkey cohort as in (B) were shown. Sleep EEG was recorded via telemetry devices as described in STAR Methods. Unpaired *t*-test was performed (ns not significant, *p < 0.05, **p < 0.01, ***p < 0.001), and data were shown as mean ± SEM.

behavior. In both approaches, we concluded that sleep and neuropsychiatric disorders found by BMAL1-deficiency were associated with the dysregulation of high-frequency neural activities.

RESULTS

BMAL1-deficiency led to distinct sleep outcomes in adult mice and cynomolgus monkeys

Circadian clock dysfunctions underlie sleep disorders in multiple features,[22–24] however a direct electroencephalogram (EEG) analysis in diurnal animals for such a correlation was rare due to the limitation of suitable models.[25] To monitor long-term sleep epochs with continuous inspection of daily activities in diurnal animals, we applied adult wild-type cynomolgus monkeys (WT monkey) and a circadian-disrupted model, BMAL1 knockout monkeys (BKO monkey)[14] for free-moving wireless recordings of EEG, locomotor activity, and body temperature under a 12-h light/12-h dark cycle (L/D)(See experimental scheme in Figure S1). With the setup, we first try to study a paradoxical condition that BMAL1 deficiency was reported to cause shorter sleep in monkeys at preadolescent age,[14] but produce the opposite outcome in mice.[19] We found the total sleep time results (ZT0-24) were consistent with earlier findings that BKO mice showed longer NREM sleep (~11%, Figure 1A), while BKO monkeys at adult age remained with sleep difficulty of about 6.5% shorter NREM sleep at the current age (Figure 1B). The excess sleep in BKO mice happened in the dark period (ZT12-24), indicating that the BKO mice were less active in the by principle-awake time (Figure 1A). Conversely, the reduced sleep in BKO monkeys occurred in the dark time, showing that the BKO monkeys were restless in the sleeping period (Figure 1B). Mild disturbance of the circadian clock via constant light illumination (L/L) did not expand the difference between WT and BKO mice, as the extended illumination triggered longer sleep for the WT mice but not further for BKO mice (Figure 1C). Notably, in the case of BKO monkeys, LL decreased their sleep time further (Figure 1D).

Diurnal EEG analyses indicated different EEG power patterns associated with circadian disturbance in BMAL1-deficient mice and monkeys

To elucidate the difference in detail, we further analyzed sleep stages in WT and BKO monkeys. Similar to the human hypnogram, the WT monkey showed clear slow-wave sleep (SWS) during the early night (Figure 2A) and exhibited lower body temperature associated with the SWS stage (Figure 2B). The EEG spectrogram from the WT monkey revealed a gradual switch from low-frequency oscillations in the nighttime to high-frequency oscillations (>30 Hz) in the daytime, as can be seen from a 24-h window (Figure 2B). Different from the clear day versus night pattern found in the male WT monkey, the male BKO monkey exhibited disrupted circadian patterns, including higher nocturnal movement, lesser SWS (Figure 2A), disorganized high-frequency oscillations (>30 Hz), and higher body temperature during the nighttime (Figure 2B). Environmental interference by L/L did not alter the diurnal EEG and body temperature patterns in the WT monkey, but largely raised high-frequency neural oscillations and body temperature in the BKO monkey during the original resting time (Figure 2B), suggesting that the circadian rhythms in the BKO monkey were easily disturbed by external changes. We observed similar circadian clock-disrupted phenotypes in another female BKO monkey that also showed dysregulated body temperature and high-frequency oscillations (Figure S2).

To study the atypical nighttime high-frequency oscillations that occurred in the BKO monkeys, we separated the 24-h EEG activities into day versus night sections and analyzed the respective EEG spectra (Figure 2C). Typically, the spectrum reveals exponentially decreased power through the increase of frequency.[26,27] The monkey EEG results, particularly the night section from WT fit well with the correlation (Figure 2C). We also noticed that under the L/D cycle, the most distinct neural activities between day and night were higher theta and gamma oscillations in the daytime. The higher theta and gamma oscillations conceivably indicated more active attention events occurred during awake.[28,29] By contrast, BKO monkeys showed peaked alpha and beta power at near 8 Hz and 15–30 Hz bands, respectively, in both day and night periods (Figures 2C and S2B). Of note, by summarizing 24-h EEG spectra of the three WT and BKO monkey pairs, we found that beta and gamma powers were higher in BKO than in WT monkeys (Figure 2D) and appeared in all stages, including awake, REM, N1/N2, SWS (Figure S3A). The results indicated that high-frequency beta and gamma oscillations are consistent EEG markers to identify BMAL1 deficiency in all stages in cynomolgus monkeys (Figure 2D).

To relate the circadian clock phenotypes in rodents, we analyzed EEG from WT and BKO mice in a parallel manner. Adult WT mice showed relatively lower body temperature and reduced high-frequency oscillation during resting in the light-on period (Figures 3A and 3B). Unlike the WT monkey results, the WT mouse presented more fragmental resting accompanied with lower body temperature during the light-off time (Figures 3A and 3B). In the BKO mice, the day versus night differences vanished, and the body temperature fluctuated largely with the occurrence of high-frequency oscillations (Figures 3A and 3B). Constant illumination L/L suppressed and delayed high-frequency oscillations in the WT mice, and in the case of BKO, led to more recurrent high-low frequency and body temperature switches (Figure 3B). In contrast to the findings in monkeys, the EEG spectra did not show obvious EEG band variance between WT and BKO mice (Figure 3C). 24-h EEG spectra identified higher theta power in BKO mice (Figure 3D), and the theta power change correlated to awake and REM sleep (Figure S3B). Interestingly, BKO mice did not show high-frequency dysregulation, revealing that BMAL1-ablation led to different outcomes on neural activities in mice and monkeys. Of note, mice showed higher beta and gamma powers than monkeys (Figure S3C). The basal differences may contribute to the dissimilar outcomes in BKO mice and monkeys.

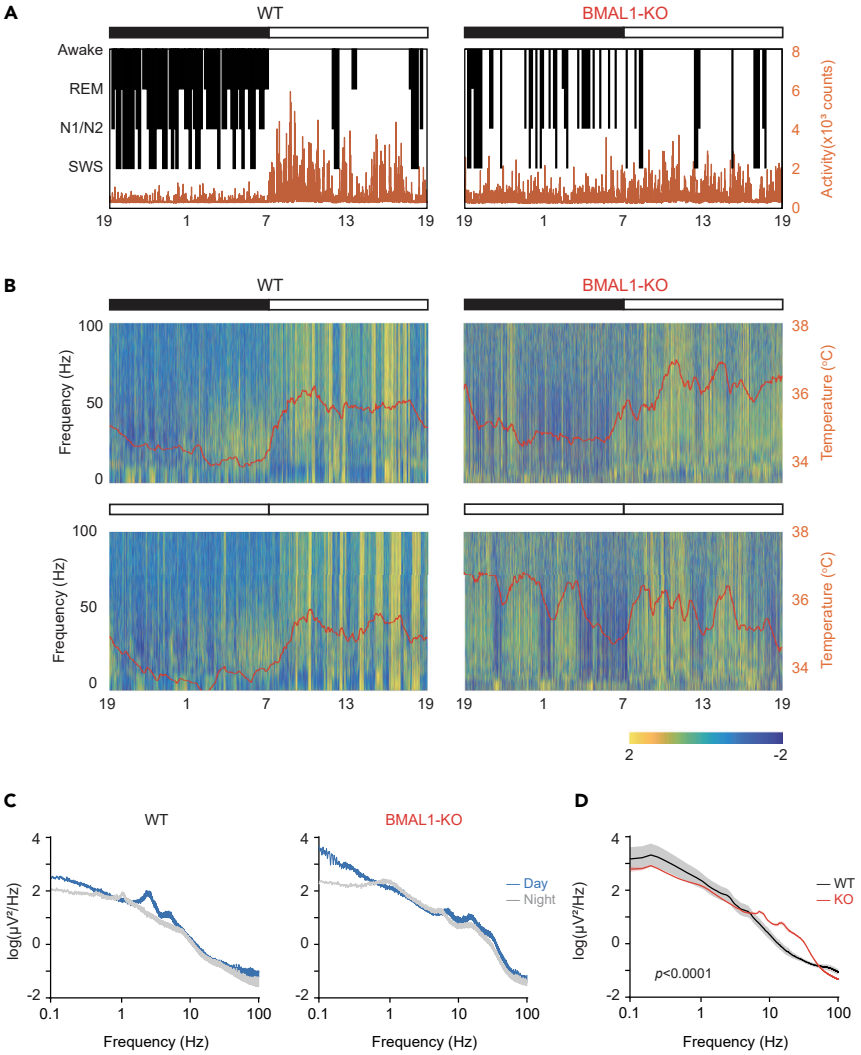

Figure 2. Diurnal activity, hypnogram and EEG spectrogram of adult cynomolgus monkeys

(A) Hypnogram and locomotion counts of a representative 5-year-old wild-type male monkey (left) and a BMAL1-KO male monkey (right) over a 24-h recording under normal 12 h light-12 h dark (L/D) cycle. Light-on (7:00-19:00) and light-off (19:00-7:00) periods are indicated and marked on top.

(B) The *Z* score EEG spectrogram and body temperature (red curve) of male WT and BMAL1-KO monkeys under L/D cycle housing, or constant illumination (L/L) housing (below).

(C) Day (blue) and night (gray) EEG power spectra of male WT and BMAL1-KO monkeys under L/D housing.

(D) EEG power spectra between WT (black curve, n = 3) and BMAL1-KO monkeys (red curve, n = 3) under L/D housing. All data were represented as mean ± SEM. Two-way ANOVA with Bonferroni correction for multiple comparison was performed, and the p values between WT and BMAL1-KO groups were shown in the insets.

To understand the day versus night EEG difference revealed from EEG spectra in monkeys (Figure 2C), we further depicted z-scored power distribution of individual EEG bands that covered delta (0.5–4 Hz), theta (4–8 Hz), alpha (8–12 Hz), beta (13–32 Hz), and gamma (>32 Hz) bands. The power distributions were displayed with separating day and night sections where in each section included power events every 2 min. We found in WT monkeys the majority of oscillating events were below the 24-h mean power for all EEG bands during the night (Figures 4A–4E). As a contrast, in the daytime, neural activities of essentially all EEG bands were above the mean power, particularly for theta and gamma power with broader distribution (Figures 4B and 4E). BKO monkeys exhibited advantageous beta and gamma power distributions above average, as could be noted in the EEG spectra as well (Figure 2C). The day-night differences of delta and alpha activities were diminished upon BMAL1 loss (Figures 4A and 4C), implicating that the consciousness level and attention-related functions might be disturbed during the circadian cycle.[30–32] Interestingly, mouse as a nocturnal model exhibited similar higher power distribution of most bands during the daytime (Figures 4F–4I), except for the gamma band (Figure 4J). In mice, the gamma band showed clear preferable activities in the light-off period in contrast to monkeys, indicating that the gamma band distinguished nocturnal-versus diurnal-active patterns better than other bands.

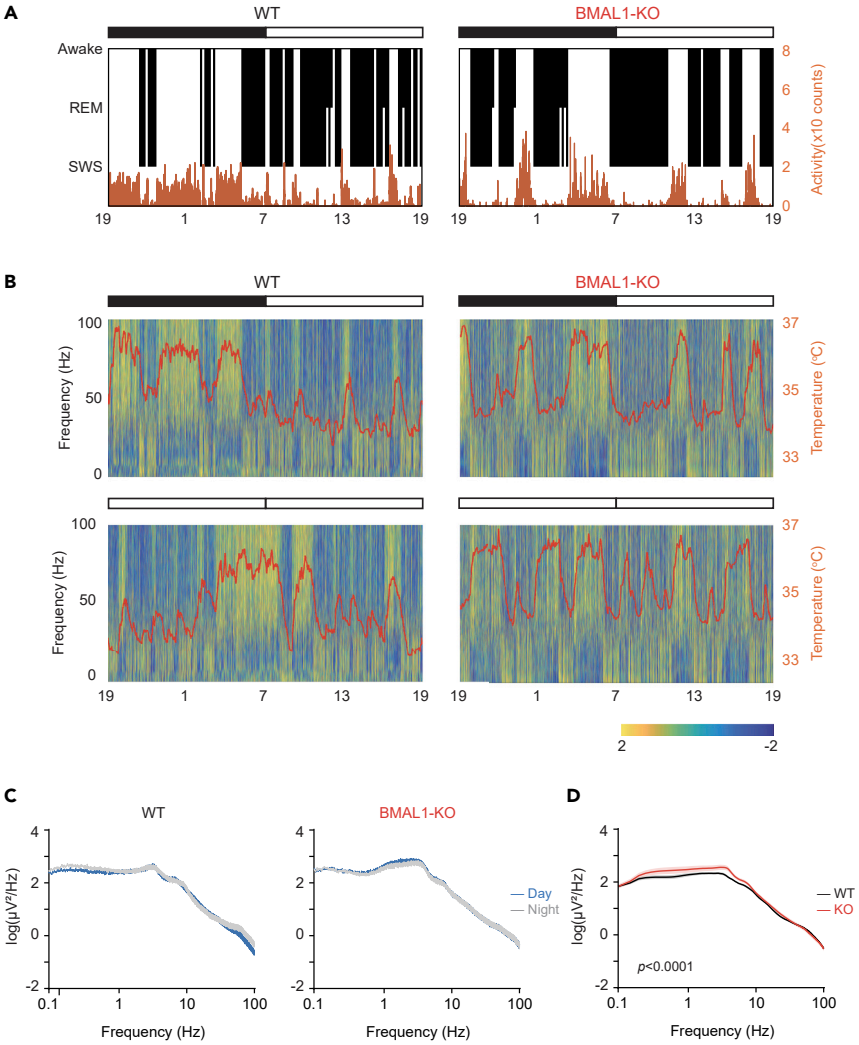

Figure 3. Diurnal activity, hypnogram and EEG spectrogram of adult mice

(A) Hypnogram and locomotion counts of a representative 4-month-old wild-type male mouse (left) and a Bmal1-KO male mouse (right) over a 24-h recording under normal 12 h light-12 h dark (L/D) cycle. Light-on (7:00-19:00) and light-off (19:00-7:00) periods are indicated on top.

(B) The *Z* score EEG spectrogram and body temperature (red curve) of male WT and Bmal1-KO mice under L/D cycle housing, or constant illumination (L/L) housing (below).

(C) Day (blue) and night (gray) EEG power spectra of male WT and Bmal1-KO mice under L/D housing.

(D) EEG power spectra between WT (black curve, n = 5) and Bmal1-KO mice (red curve, n = 5) under L/D housing. All data were represented as mean ± SEM. Two-way ANOVA with Bonferroni correction for multiple comparison was performed, and the p values between WT and BMAL1-KO groups were shown in the insets.

Devoid of BMAL1 abolished the day-night differences of all bands in mice. The varying results between monkey and mouse pointed out that clock dysfunction could generate diverse impacts on neural oscillations among species. The dissimilarities could be caused by many factors such as brain size and cognitive complexity.[8]

Day-night EEG divergence identified dysregulated high-frequency oscillations in BMAL1-deficient mice and monkeys

To verify the frequency range that differed significantly between day and night, we next applied Kullback-Leibler divergence (KLD),[21] also known as relative entropy, for the day-night test over a 24-h period. We first separated the daytime EEG and nighttime EEG sections, then accumulated the analysis time that centered at the light-off moment 19:00 till the full section of 12 h (Figure S4A). We found KLD of representative delta, theta, alpha, beta, gamma, and high-gamma bands at 3, 6, 12, 25, 50, and 100 Hz, respectively, exhibited different significant patterns over time (Figure S4B). While delta and theta bands reached the highest divergence in the first 2 h in the WT monkeys, possibly reflecting the best sleep period, the high gamma band required more than 3h day plus 3h night sections to reveal a steady outcome (Figure S4C). To tell the difference in detail, we then performed a full-frequency KLD scan (0–100 Hz) of including a complete 24h, 12h

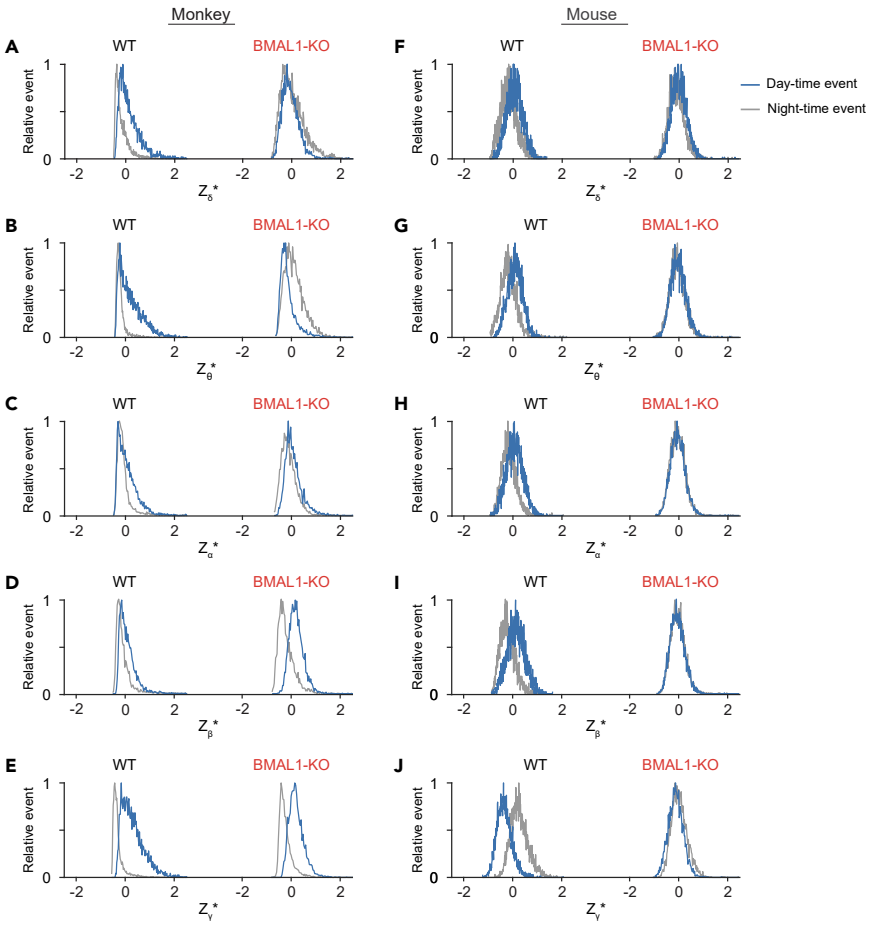

Figure 4. Diurnal EEG power analysis of day-night distribution in monkeys and mice

(A) The *Z* score delta (0.5–4 Hz), (B) theta (4–8 Hz), (C) alpha (8–12 Hz), (D) beta (13–32 Hz), and (E) gamma (32–100 Hz) band power distribution in a day (blue) versus night (gray) comparison of monkey (left, WT n = 3, or BKO n = 3) under L/D condition. Mouse EEG band power distributions were analyzed and shown in (F) delta, (G) theta, (H) alpha, (I) beta, and (J) gamma waves (right, WT n = 5, or BKO n = 5). The power distributions were revealed by separating day and night sections, in each section summarized power events every 2-min then normalized the highest event count as 1.

day-12h night EEG. We found the full-frequency KLD test offered a clear separation of the EEG spectral power of WT monkeys from the BKO monkeys under normal L/D condition (Figure 5A). The EEG spectral power of WT monkey KLD troughed at the beta band (~20 Hz), then showed growing day-night divergence with increasing frequency (Figure 5A). The gamma band, particularly the high gamma oscillations (60–100 Hz), displayed a higher KLD value than other bands, indicating that gamma power was tightly regulated in a day versus night manner. Notably, the BKO monkey showed an opposite pattern of the KLD curve, which peaked at the beta band (~30 Hz) and revealed a persisted low KLD in the high gamma band (Figure 5A). The diminished day-night divergence in the gamma band and peaked KLD in the beta band stated that high-frequency dysregulation is a prominent marker for circadian clock disorder.

The sharp KLD difference between circadian clock-normal and -dysfunctional situations proposed that KLD analysis might be a sensitive measurement to tell circadian clock dysfunction and sleep disturbance. Indeed, under L/L housing, KLD of essentially all EEG bands declined in WT and BKO monkeys and showed a compressed day-night contrast (Figure 5B). To further test whether the KLD is suitable to reflect mild sleep treatment, we included melatonin in our test. Melatonin is commonly used to alleviate jet lag and is a milder safer alternative to other sleeping aids such as benzodiazepines.[33–35] We found under L/L condition, the WT monkeys with receiving oral administration of 2 mg/kg melatonin at 7 p.m. showed improved KLD in high-frequency bands (Figure 5C). Melatonin showed no significant effect in BKO monkeys (Figure 5D, p = 0.1814, two-way ANOVA), possibly due to a defective melatonin signaling that occurred upon BMAL1 loss. Based on the results, we found circadian KLD analysis is a decent method to evaluate sleep and circadian disorders. As the divergence can be revealed from as short as 2h day-2h night EEG data (Figures S4B and S4C), circadian KLD appeared to be more convenient than the standard sleep analysis, which required a complete period of sleep EEG recording.

We further applied the KLD method to measure sleep patterns in mice. In the day versus night KLD, we found delta, theta, alpha, and gamma bands had higher day-night divergence in WT mice under L/D and D/D conditions, while L/L inhibited the circadian preference

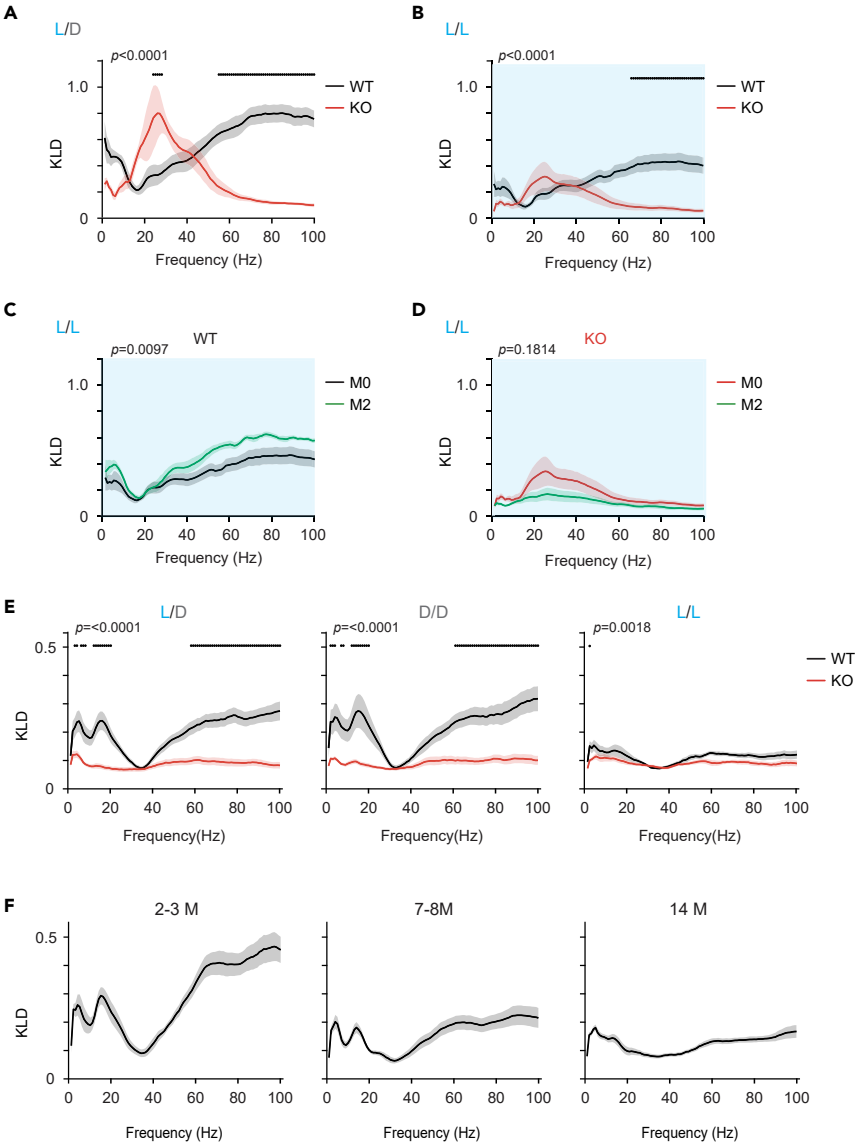

Figure 5. Diurnal EEG divergence analysis of day-night distribution in monkeys and mice

(A) Kullback-Leibler divergence (KLD) of diurnal monkey EEG over frequency bands (0-100Hz) under the condition of L/D. KLD of night versus day EEG powers were analyzed. Black dots on top indicate with significant difference ($p < 0.05$, *t*-test) at the corresponding frequency band between WT (black curve, n = 3) and BMAL1-KO monkeys (red curve, n = 3).

(B) KLD analysis of WT versus BKO monkey EEG recorded under constant illumination (L/L) housing.

(C) KLD analysis of WT monkey EEG under L/L housing with (green curve, M2) or without (black curve, M0) 2 mg/kg melatonin treatment.

(D) KLD analysis of BKO monkey EEG under L/L housing with (green curve, M2) or without (red curve, M0) 2 mg/kg melatonin treatment.

(E) KLD analysis of WT (black curve, n = 5) and BKO mice (red curve, n = 5) EEG that were recorded under standard (L/D), all dark (D/D), or constant illumination (L/L) housing conditions.

(F) KLD analysis of WT male mice at 2-3-month-old (n = 6), 7-8-month-old (n = 6), and 14-month-old (n = 6) under standard L/D housing condition. All data were represented as mean ± SEM. Two-way ANOVA with Bonferroni correction for multiple comparison was performed, and the p values between indicated groups were shown in the insets. Black dots on insets indicated with significant difference ($p < 0.05$, Bonferroni-adjusted significance).

(Figure 5E). In all housing conditions, BKO mice did not exhibit decent divergence in all EEG bands similar to BKO monkeys, confirming that BMAL1 is essential for partitioning day-night neural activities in both model organisms. It is unclear to us what caused the marked KLD change in the beta band in BKO monkeys, while the signature is absent in BKO mice.

Lastly, since KLD is useful in detecting the strength of circadian clock, we next tested its application for examining diurnal EEG changes at different ages, as circadian clock robustness is recognized to deteriorate with aging.[36–38] We carried out EEG recordings in mouse cohorts

that were grouped into three different adult ages and found the young adults (2-3 month-old) displayed higher divergence, particularly in the gamma bands (Figure 5F). The day-night difference became unstable at 7–8 months of age and deteriorated evidently at 14 months of age. Notably, regular sleep analysis showed only subtle differences among the adult groups (Figure S5), indicating that the day-night KLD could serve as a sensitive measurement to reflect brain oscillation states upon age progression. Together, these results demonstrated that the day-night differences of high-frequency oscillations are good markers for determining the strength of circadian rhythms in contexts including BMAL1 deficit, illumination changes, and aging.

Dysregulated beta and gamma power bands are potential biomarkers to relate psychiatric phenotypes in BMAL1-deficient monkeys

As BMAL1-deficiency led to sleep disruption and psychiatric disorders,[14,20] we next tested the possibility of using the neural oscillation differences between WT and BKO monkeys to correlate the occurrence of psychiatric behaviors. Given that dysregulated beta and gamma oscillations were notably found in BKO monkeys during the 24-h diurnal cycle (Figures 2C, 2D, and 5A), we then focused on these bands for their dynamic changes in a brief period that coupled to a situation of encountering a novel environment. In a short EEG recording of having 10-min free-exploring and 5-min experimenter-presence condition (Figure 6A), we could detect elevated beta and gamma oscillations in the range of ~10–50 Hz in BKO monkeys (Figure 6B). During the 15-min stay, we found the WT monkeys explored lively in the novel cage. In contrast, the BKO monkeys showed spontaneously occurring abnormal phenotypes, including fear of exploring, curling up, delusion-like, and even self-injuring behaviors in the unacquainted environment (Figure 6C; Videos S1, S2, and S3). The abnormal phenotypes were aggravated by the novel environment as the BKO monkeys showed less self-injuring and delusion-like events, and no curl-up behavior in their home cages (Figure S6). By summarizing 10-s band power every 2-Hz with correlating to the behavioral status, we found band powers were generally raised during abnormal behavioral events compared to normal (Figures 6D and 6E). Among those with higher significance were beta bands in 26–31 Hz, gamma bands in 45–50 Hz, and a narrow fraction of alpha bands in 10–12 Hz (Figure 6D). In the three band sections, alpha bands correlated more with self-injuring behaviors than curl-up and delusion-like events. Raised gamma power of 45–50 Hz indicated more of the curl-up and delusion-like events. Notably, the high beta power of 26–31 Hz was associated with all three abnormal behaviors, as also agreed by AUC scoring (Figure S7), and the power amplitude increased most evidently amongst the three EEG band sections (Figure 6E). To examine the finding that 26–31 Hz power change was useful to mark psychotic behaviors, we applied the female BKO monkey that showed the most severe delusion-like behaviors triggered by the novel cage for a single dose of antipsychotic Aripiprazole treatment, then inspected the alterations in neural oscillations and delusion-like events. We found Aripiprazole was able to ease the occurrence of delusion-like events and brought down 26–31 Hz beta power and 42–50 Hz gamma power (Figures 6F and S8). We further inspected depression-like behaviors in BKO mice. As WT and BKO mice did not show apparent behavioral differences in the new cage, we tried to trigger depression-like behaviors via tail suspension and open field tests in BKO mice. Interestingly, we found delta, theta, and alpha powers, but not beta power, were elevated during tail suspension immobile time and open field outer zone traveling (Figure S9). The results suggested that stress-related neural biomarkers are distinctive between BMAL1-deficient mice and monkeys. The dysregulated 26–31 Hz beta power is a unique biomarker to designate neuropsychiatric events in BKO monkeys.

DISCUSSION

Our study demonstrated that high-frequency neural activity dysregulation is a marked phenotype associated with BMAL1-deficiency. The results also proposed new neural activity-based measures that may facilitate diagnoses of sleep complaints and psychiatric disorders. In the case of sleep analysis, we showed the sleep homeostatic score, i.e., KLD of diurnal EEG, is a convenient way to present sleep quality. Standard sleep analysis reports sleep quantity. The AASM scoring manual standardizes the sleep recording method and scoring rules in great detail,[39] by which to describe essentially all sleep-related phenomena. The recommendations include but are not limited to the application of EMG, ECG, and EOG electrodes at proper positions, the acquisition of respiratory signals, and the steps of EEG analysis from data filtering to final staging. The detailed descriptions are important for sleep characterization and staging, yet unavoidably increase the processes and time in order to meet all the criteria, at the same time demand well-trained staffs to operate the procedures properly. In the current study, we found that the KLD score is helpful in presenting sleep homeostasis with reduced requirement of EEG electrode and recording time. Different from traditional sleep classifications, the method does not focus on low-frequency oscillations and sleep staging within the night period but senses the divergence of high-frequency oscillations of night-day periods to determine the sleep homeostatic state. The KLD amplitude can be revealed in a short, 4-h EEG recording, which covers 2-h awake and 2-h sleep section each (Figure S4C). The flexible recording time with single electrode requirement could simplify the process of sleep evaluation in comparison to standard sleep EEG recording, which generally needs several electrodes to stay well-connected throughout the entire recording night. The simple procedure proposed here could facilitate the use of circadian EEG as a regular home-based test, and with KLD analysis, to obtain an objective circadian fitness score representing resting quality. Although loss the information on total sleep time, REM, and NREM (N1-3) sleep, the KLD method could be applied as an alternative measure to study confusing situations such as healthy subjects with considerably shorter sleep meanwhile sustaining good physical condition and cognitive functions,[40] or long sleepers who find troubles in claiming sufficient rest.[41] The argument is also valid in comparing the BMAL1-ablated situation, which resulted in shorter sleep in the monkey,[14] but longer in the mouse model[19] (Figure 1), nevertheless collectively should be considered as a compromised state of resting, signified by the loss of diurnal divergence in gamma oscillations.

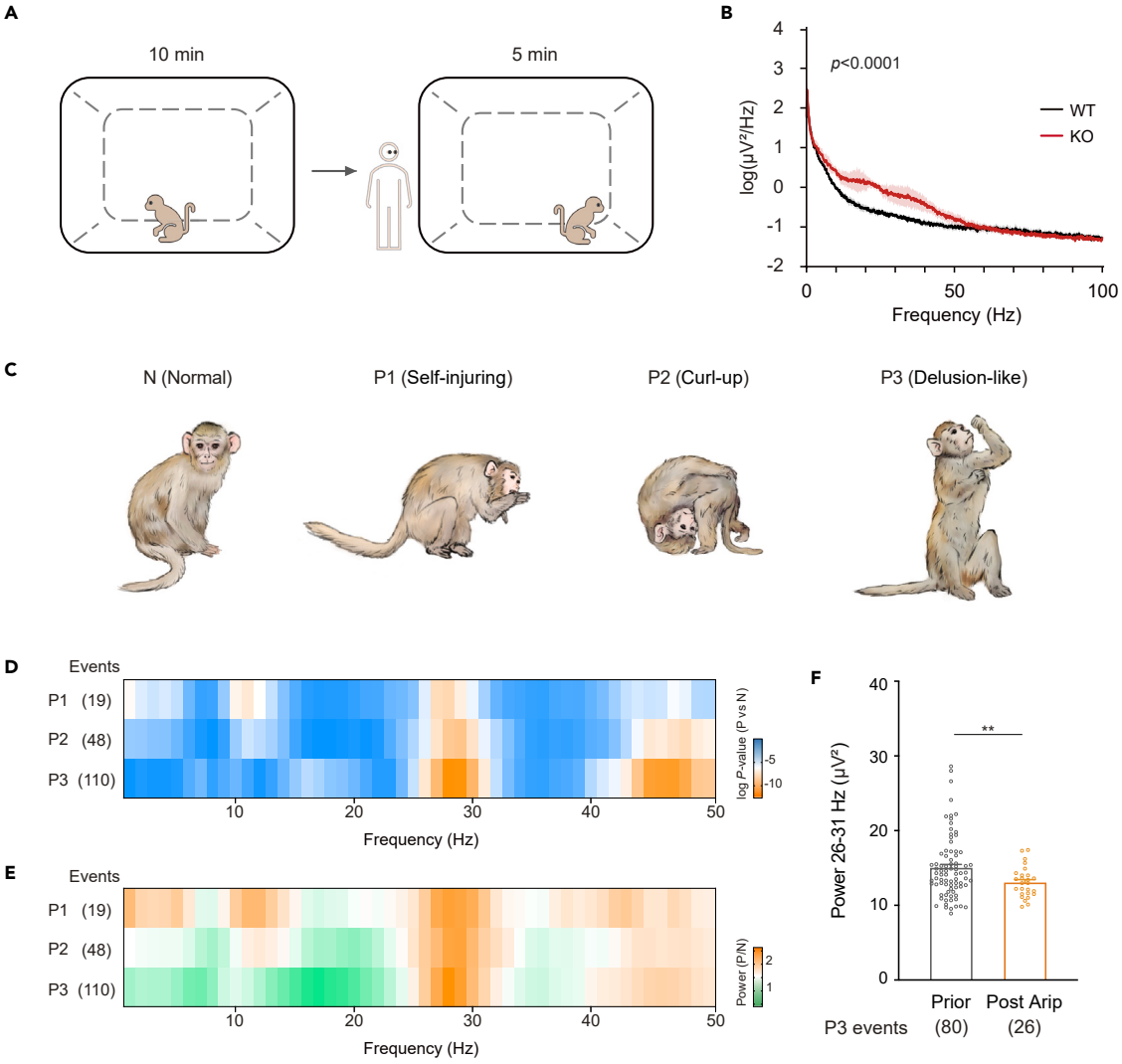

Figure 6. Identifying neural biomarkers for psychiatric behaviors in BMAL1-KO monkeys

(A) Experimental setting of 10-min novel environment exploration followed by 5-min behavior response with human presence.

(B) EEG power spectra of WT (black curve, n = 3) and BMAL1-KO (red curve, n = 3) monkeys during 15-min exploration. All data were represented as mean ± SEM. Two-way ANOVA with Bonferroni correction for multiple comparison was performed, and the p values between WT and BMAL1-KO groups were shown in the insets.

(C) Representing behavioral features occurred in the novel cage, including normal (N) showing relaxed posture, abnormal actions such as self-injuring (P1), curl up (P2), and delusion-like (P3) phenotypes. Source results were provided in supplemental information. See also Videos S1, S2, and S3.

(D) EEG band power differences of comparing abnormal behaviors P1, P2, P3 to normal events, respectively, summarized from 15-min recordings of three BKO monkeys. 10-s EEG power events were viewed in 2-Hz window scan (1–50 Hz), with relating to the behavioral status. Unpaired *t*-test was performed, and significances were shown. Total abnormal events from three BMAL1-KO monkeys were indicated.

(E) EEG power changes of P1, P2, P3 compared to normal. Fold changes were shown.

(F) EEG power change of 26–31 Hz in the female BKO monkey before and after Aripiprazole (0.1 mg/kg) treatment (Post Arip). Events were summarized every 10-s from 15-min recording. Delusion-like events in Prior = 80, Post Arip = 26. Unpaired *t*-test was performed (**p < 0.01), and data were shown as mean ± SEM.

The KLD analysis also indicated different diurnal EEG signatures between mouse and monkey. Monkey displayed less fragmental awake-sleep switch during resting (Figure 2B) and exhibited clear day-night divergence in gamma bands (Figure 5A). Mouse revealed more low-high frequency switches even during resting, which resulted in lower KLD scores in general (Figure 5E). Interestingly, we found the lowest day-night divergence happened in beta bands in healthy adult monkeys and mice. Monkeys exhibited low KLD near 20 Hz (Figure 5A), while in mice, the low KLD occurred near 30 Hz within the transition of beta and gamma bands (Figure 5E). This indicated that mice maintain constant neural oscillations near 30 Hz in both awake and sleep, possibly facilitating rapid responses to threats during sleep. The low KLD point appeared to be characteristic within species, as the change in illumination program or age did not alter the position (Figures 5A, 5B, 5E, and 5F). KLD

amplitudes of delta, theta, alpha, and high gamma bands were responsive to environment and age, especially the high gamma oscillations were sensitive in both animal models. Interestingly, we noticed that the KLD curve may help to uncover a circadian clock-related biomarker for aging (Figure 5F). Of note, due to the differences in KLD pattern and the outcome caused by BMAL1-deficiency recognized between mouse and monkey, the application of mouse biomarkers for representing human brain diseases and the subsequent translational purposes should be carefully examined.

In the case of EEG biomarkers for psychiatric phenotypes, we found that the elevated beta power in 26–31 Hz and gamma power in 45–50 Hz were associated with the occurrence of abnormal behaviors. The conclusion is coherent with the observation of high-frequency power dysregulation from 24-h EEG spectrogram and KLD curve in BKO monkeys. Approaches for identifying EEG biomarkers, e.g., EEG power spectrum, evoked potentials, and functional connectivity, are typically inspected via eye open/close resting states or visual/auditory responses with multi-channel EEG setting.[42,43] The former revealed a predisposed power difference, and the latter reflected neural responses and the amplitudes during tasks. The specificity of the resulting EEG biomarkers often varied among studies that could be influenced by the procedures of EEG recording and analysis, the selection of participants, and the characterization of disease types.[42,44] Also, as many behavioral symptoms are shared in different psychiatric disorders, including anxiety, bipolar disorder, schizophrenia, depression, etc., that further increases the difficulty of discovering disease-specific EEG biomarkers. In the study, we sought to circumvent the issues with simplified protocol in an animal model, i.e., the BMAL1-deficient monkey model, that is convenient for abnormal behavior classification. We ignored the task-based neural responses among electrodes but followed band power changes in a free-moving context with mild disturbances such as encountering an unfamiliar environment and person. The setting can be viewed as events common to lives and thus did not cause discomfort for WT monkeys, nevertheless, it was sufficient to trigger peculiar behaviors in BKO monkeys. Also, by focusing on the change of band power related to normal versus major irregular behaviors, the resulting biomarkers aim to designate respective behavioral abnormality rather than the determination of disease type. The method could be useful in a few aspects. First, the assay measures responses by instinct so does not require any pre-training or learning process for tasks that may affect the efficiency of data collection and the interpretation of data. Second, the approach scores EEG power fold-change within individual animal, emphasizes on the contrast of power events between normal and abnormal behaviors, and therefore omits the comparison of band power to assumed control that may introduce heterogeneity while defining normal. Third, the method focuses on abnormal event counts and the associated band power changes, which grades only the two connections to present abnormal severity. The assessment could simplify the process of testing antidepressant efficacy. Also, the biomarkers could show symptom-oriented outcomes separately upon antidepressant treatment instead of reviewing the overall drug effects on one particular disease. Finally, considering the strong association of circadian clock dysfunction to sleep disorders, psychiatric and neurodegenerative diseases,[3,45–53] circadian clock related strategies such as diurnal KLD assessment, neural biomarker identification and other designs in the future are likely to foster the findings of more accurate disease biomarkers and therapeutic methods for multiple brain diseases.

Limitations of the study

It is important to note that the conclusions of high-frequency neural activity dysregulation and depression-associated EEG biomarkers were derived from only three BMAL1-ablated monkeys. More mechanistic demonstrations relating circadian clock disturbance to psychiatric disorders should be conducted to extend the findings.

STAR★METHODS

Detailed methods are provided in the online version of this paper and include the following:

- KEY RESOURCES TABLE
- RESOURCE AVAILABILITY
  - Lead contact
  - Materials availability
  - Data and code availability
- EXPERIMENTAL MODEL AND STUDY PARTICIPANT DETAILS
  - Cynomolgus monkey and mouse
- METHOD DETAILS
  - Electroencephalography recording
  - EEG data processing, filtering, and artifact rejection
  - Kullback–Leibler divergence
  - Behavioral recordings in novel environment
  - Behavioral recordings in mice
- QUANTIFICATION AND STATISTICAL ANALYSIS

SUPPLEMENTAL INFORMATION

Supplemental information can be found online at https://doi.org/10.1016/j.isci.2024.109381.

ACKNOWLEDGMENTS

This work was supported by grants from the National Natural Science Foundation of China (82021001 to H-C.C), the National Science and Technology Innovation 2030 Major Program (2021ZD0200904 to H-C.C.), Lingang Laboratory (LG202106-02-02 to H-C.C. and LG202106-02-04 to Y-C.T.), the Strategic Priority Research Program of the Chinese Academy of Sciences (XDB32060200 to H-C.C.), and the Shanghai Municipal Science and Technology Major Project (2018SHZDZX05 to H-C.C.). The authors acknowledge the members of Songjiang Non-human Primate Facility of the CAS Center for Excellence in Brain Science and Intelligence Technology for their assistance in animal care.

AUTHOR CONTRIBUTIONS

Methodology, Y.S., J.J., Y.-C.T., and H.-C.C.; investigation, Y.S., M.Z., N.X., X.Z., and H.S.; data analysis, Y.S., H.S., Y.-C.T., and H.-C.C.; resources, Y.W., Y.L., Y. N., Q.L., and Q.S.; conceptualization and supervision, H.-C.C.

DECLARATION OF INTERESTS

The authors declare no competing interests.

Received: September 25, 2023
Revised: January 29, 2024
Accepted: February 27, 2024
Published: March 1, 2024

REFERENCES

1. Bass, J., and Takahashi, J.S. (2010). Circadian integration of metabolism and energetics. Science *330*, 1349–1354. https://doi.org/10.1126/science.1195027.
2. Liu, F., and Chang, H.C. (2017). Physiological links of circadian clock and biological clock of aging. Protein Cell *8*, 477–488. https://doi.org/10.1007/s13238-016-0366-2.
3. Mattis, J., and Sehgal, A. (2016). Circadian Rhythms, Sleep, and Disorders of Aging. Trends Endocrinol. Metab. *27*, 192–203. https://doi.org/10.1016/j.tem.2016.02.003.
4. Lamont, E.W., Legault-Coutu, D., Cermakian, N., and Boivin, D.B. (2007). The role of circadian clock genes in mental disorders. Dialogues Clin. Neurosci. *9*, 333–342.
5. Charrier, A., Olliac, B., Roubertoux, P., and Tordjman, S. (2017). Clock Genes and Altered Sleep-Wake Rhythms: Their Role in the Development of Psychiatric Disorders. Int. J. Mol. Sci. *18*, 938. https://doi.org/10.3390/ijms18050938.
6. Musiek, E.S., and Holtzman, D.M. (2016). Mechanisms linking circadian clocks, sleep, and neurodegeneration. Science *354*, 1004–1008.
7. Logan, R.W., and McClung, C.A. (2019). Rhythms of life: circadian disruption and brain disorders across the lifespan. Nat. Rev. Neurosci. *20*, 49–65. https://doi.org/10.1038/s41583-018-0088-y.
8. Buzsáki, G., Logothetis, N., and Singer, W. (2013). Scaling brain size, keeping timing: evolutionary preservation of brain rhythms. Neuron *80*, 751–764. https://doi.org/10.1016/j.neuron.2013.10.002.
9. Nunn, C.L., and Samson, D.R. (2018). Sleep in a comparative context: Investigating how human sleep differs from sleep in other primates. Am. J. Phys. Anthropol. *166*, 601–612. https://doi.org/10.1002/ajpa.23427.
10. Nelson, E.E., and Winslow, J.T. (2009). Non-human primates: model animals for developmental psychopathology. Neuropsychopharmacology *34*, 90–105. https://doi.org/10.1038/npp.2008.150.
11. Izpisua Belmonte, J.C., Callaway, E.M., Caddick, S.J., Churchland, P., Feng, G., Homanics, G.E., Lee, K.F., Leopold, D.A., Miller, C.T., Mitchell, J.F., et al. (2015). Brains, genes, and primates. Neuron *86*, 617–631. https://doi.org/10.1016/j.neuron.2015.03.021.
12. Jennings, C.G., Landman, R., Zhou, Y., Sharma, J., Hyman, J., Movshon, J.A., Qiu, Z., Roberts, A.C., Roe, A.W., Wang, X., et al. (2016). Opportunities and challenges in modeling human brain disorders in transgenic primates. Nat. Neurosci. *19*, 1123–1130. https://doi.org/10.1038/nn.4362.
13. Bunger, M.K., Wilsbacher, L.D., Moran, S.M., Clendenin, C., Radcliffe, L.A., Hogenesch, J.B., Simon, M.C., Takahashi, J.S., and Bradfield, C.A. (2000). Mop3 is an essential component of the master circadian pacemaker in mammals. Cell *103*, 1009–1017.
14. Qiu, P., Jiang, J., Liu, Z., Cai, Y., Huang, T., Wang, Y., Liu, Q., Nie, Y., Liu, F., Cheng, J., et al. (2019). BMAL1 knockout macaque monkeys display reduced sleep and psychiatric disorders. Natl. Sci. Rev. *6*, 87–100. https://doi.org/10.1093/nsr/nwz002.
15. Liu, Z., Cai, Y., Liao, Z., Xu, Y., Wang, Y., Wang, Z., Jiang, X., Li, Y., Lu, Y., Nie, Y., et al. (2019). Cloning of a gene-edited macaque monkey by somatic cell nuclear transfer. Natl. Sci. Rev. *6*, 101–108. https://doi.org/10.1093/nsr/nwz003.
16. Marcheva, B., Ramsey, K.M., Buhr, E.D., Kobayashi, Y., Su, H., Ko, C.H., Ivanova, G., Omura, C., Mo, S., Vitaterna, M.H., et al. (2010). Disruption of the clock components CLOCK and BMAL1 leads to hypoinsulinaemia and diabetes. Nature *466*, 627–631. https://doi.org/10.1038/nature09253.
17. Kondratov, R.V., Kondratova, A.A., Gorbacheva, V.Y., Vykhovanets, O.V., and Antoch, M.P. (2006). Early aging and age-related pathologies in mice deficient in BMAL1, the core componentof the circadian clock. Genes Dev. *20*, 1868–1873.
18. Nguyen, K.D., Fentress, S.J., Qiu, Y., Yun, K., Cox, J.S., and Chawla, A. (2013). Circadian gene Bmal1 regulates diurnal oscillations of Ly6C(hi) inflammatory monocytes. Science *341*, 1483–1488. https://doi.org/10.1126/science.1240636.
19. Laposky, A., Easton, A., Dugovic, C., Walisser, J., Bradfield, C., and Turek, F. (2005). Deletion of the mammalian circadian clock gene BMAL1/Mop3 alters baseline sleep architecture and the response to sleep deprivation. Sleep *28*, 395–409.
20. Landgraf, D., Long, J.E., Proulx, C.D., Barandas, R., Malinow, R., and Welsh, D.K. (2016). Genetic Disruption of Circadian Rhythms in the Suprachiasmatic Nucleus Causes Helplessness, Behavioral Despair, and Anxiety-like Behavior in Mice. Biol. Psychiatry *80*, 827–835. https://doi.org/10.1016/j.biopsych.2016.03.1050.
21. Kullback, S., and Leibler, R.A. (1951). On Information and Sufficiency. Ann. Math. Statist. *22*, 79–86.
22. Sehgal, A., and Mignot, E. (2011). Genetics of sleep and sleep disorders. Cell *146*, 194–207. https://doi.org/10.1016/j.cell.2011.07.004.
23. Hsu, P.K., Ptáček, L.J., and Fu, Y.H. (2015). Genetics of human sleep behavioral phenotypes. Methods Enzymol. *552*, 309–324. https://doi.org/10.1016/bs.mie.2014.10.046.
24. Cederroth, C.R., Albrecht, U., Bass, J., Brown, S.A., Dyhrfjeld-Johnsen, J., Gachon, F., Green, C.B., Hastings, M.H., Helfrich-Förster, C., Hogenesch, J.B., et al. (2019). Medicine in the Fourth Dimension. Cell Metab. *30*, 238–250. https://doi.org/10.1016/j.cmet.2019.06.019.
25. Mure, L.S., Le, H.D., Benegiamo, G., Chang, M.W., Rios, L., Jillani, N., Ngotho, M., Kariuki, T., Dkhissi-Benyahya, O., Cooper, H.M., and Panda, S. (2018). Diurnal transcriptome atlas of a primate across major neural and peripheral tissues. Science *359*, eaao0318. https://doi.org/10.1126/science.aao0318.
26. Donoghue, T., Haller, M., Peterson, E.J., Varma, P., Sebastian, P., Gao, R., Noto, T., Lara, A.H., Wallis, J.D., Knight, R.T., et al. (2020). Parameterizing neural power spectra into periodic and aperiodic components. Nat. Neurosci. *23*, 1655–1665. https://doi.org/10.1038/s41593-020-00744-x.

27. Voytek, B., Kramer, M.A., Case, J., Lepage, K.Q., Tempesta, Z.R., Knight, R.T., and Gazzaley, A. (2015). Age-Related Changes in 1/f Neural Electrophysiological Noise. J. Neurosci. *35*, 13257–13265. https://doi.org/10.1523/JNEUROSCI.2332-14.2015.
28. Köster, M., and Gruber, T. (2022). Rhythms of human attention and memory: An embedded process perspective. Front. Hum. Neurosci. *16*, 905837. https://doi.org/10.3389/fnhum.2022.905837.
29. Fernandez-Ruiz, A., Sirota, A., Lopes-Dos-Santos, V., and Dupret, D. (2023). Over and above frequency: Gamma oscillations as units of neural circuit operations. Neuron *111*, 936–953. https://doi.org/10.1016/j.neuron.2023.02.026.
30. Uhlhaas, P.J., and Singer, W. (2010). Abnormal neural oscillations and synchrony in schizophrenia. Nat. Rev. Neurosci. *11*, 100–113. https://doi.org/10.1038/nrn2774.
31. Frohlich, J., Toker, D., and Monti, M.M. (2021). Consciousness among delta waves: a paradox? Brain *144*, 2257–2277. https://doi.org/10.1093/brain/awab095.
32. Doesburg, S.M., Green, J.J., McDonald, J.J., and Ward, L.M. (2009). From local inhibition to long-range integration: a functional dissociation of alpha-band synchronization across cortical scales in visuospatial attention. Brain Res. *1303*, 97–110. https://doi.org/10.1016/j.brainres.2009.09.069.
33. Altun, A., and Ugur-Altun, B. (2007). Melatonin: therapeutic and clinical utilization. Int. J. Clin. Pract. *61*, 835–845. https://doi.org/10.1111/j.1742-1241.2006.01191.x.
34. Chen, Z., Yoo, S.H., and Takahashi, J.S. (2018). Development and Therapeutic Potential of Small-Molecule Modulators of Circadian Systems. Annu. Rev. Pharmacol. Toxicol. *58*, 231–252. https://doi.org/10.1146/annurev-pharmtox-010617-052645.
35. Stein, R.M., Kang, H.J., McCorvy, J.D., Glatfelter, G.C., Jones, A.J., Che, T., Slocum, S., Huang, X.P., Savych, O., Moroz, Y.S., et al. (2020). Virtual discovery of melatonin receptor ligands to modulate circadian rhythms. Nature *579*, 609–614. https://doi.org/10.1038/s41586-020-2027-0.
36. Nakamura, T.J., Nakamura, W., Yamazaki, S., Kudo, T., Cutler, T., Colwell, C.S., and Block, G.D. (2011). Age-related decline in circadian output. J. Neurosci. *31*, 10201–10205. https://doi.org/10.1523/JNEUROSCI.0451-11.2011.
37. Acosta-Rodríguez, V.A., Rijo-Ferreira, F., Green, C.B., and Takahashi, J.S. (2021). Importance of circadian timing for aging and longevity. Nat. Commun. *12*, 2862. https://doi.org/10.1038/s41467-021-22922-6.
38. Chang, H.C., and Guarente, L. (2013). SIRT1 mediates central circadian control in the SCN by a mechanism that decays with aging. Cell *153*, 1448–1460. https://doi.org/10.1016/j.cell.2013.05.027.
39. Berry, R.B., Brooks, R., Gamaldo, C., Harding, S.M., Lloyd, R.M., Quan, S.F., Troester, M.T., and Vaughn, B.V. (2017). AASM Scoring Manual Updates for 2017 (Version 2.4). J. Clin. Sleep Med. *13*, 665–666. https://doi.org/10.5664/jcsm.6576.
40. Shi, G., Wu, D., Ptáček, L.J., and Fu, Y.H. (2017). Human genetics and sleep behavior. Curr. Opin. Neurobiol. *44*, 43–49. https://doi.org/10.1016/j.conb.2017.02.015.
41. Castelnovo, A., Ferri, R., Punjabi, N.M., Castronovo, V., Garbazza, C., Zucconi, M., Ferini-Strambi, L., and Manconi, M. (2019). The paradox of paradoxical insomnia: A theoretical review towards a unifying evidence-based definition. Sleep Med. Rev. *44*, 70–82. https://doi.org/10.1016/j.smrv.2018.12.007.
42. Newson, J.J., and Thiagarajan, T.C. (2018). EEG Frequency Bands in Psychiatric Disorders: A Review of Resting State Studies. Front. Hum. Neurosci. *12*, 521. https://doi.org/10.3389/fnhum.2018.00521.
43. Fong, D.H.C., Cohen, A., Boughton, P., Raftos, P., Herrera, J.E., Simon, N.G., and Putrino, D. (2020). Steady-State Visual-Evoked Potentials as a Biomarker for Concussion: A Pilot Study. Front. Neurosci. *14*, 171. https://doi.org/10.3389/fnins.2020.00171.
44. Zhang, Y., Wu, W., Toll, R.T., Naparstek, S., Maron-Katz, A., Watts, M., Gordon, J., Jeong, J., Astolfi, L., Shpigel, E., et al. (2021). Identification of psychiatric disorder subtypes from functional connectivity patterns in resting-state electroencephalography. Nat. Biomed. Eng. *5*, 309–323. https://doi.org/10.1038/s41551-020-00614-8.
45. Ben Simon, E., Rossi, A., Harvey, A.G., and Walker, M.P. (2020). Overanxious and underslept. Nat. Hum. Behav. *4*, 100–110. https://doi.org/10.1038/s41562-019-0754-8.
46. Helfrich, R.F., Mander, B.A., Jagust, W.J., Knight, R.T., and Walker, M.P. (2018). Old Brains Come Uncoupled in Sleep: Slow Wave-Spindle Synchrony, Brain Atrophy, and Forgetting. Neuron *97*, 221–230.e4. https://doi.org/10.1016/j.neuron.2017.11.020.
47. Jansen, P.R., Watanabe, K., Stringer, S., Skene, N., Bryois, J., Hammerschlag, A.R., de Leeuw, C.A., Benjamins, J.S., Muñoz-Manchado, A.B., Nagel, M., et al. (2019). Genome-wide analysis of insomnia in 1,331,010 individuals identifies new risk loci and functional pathways. Nat. Genet. *51*, 394–403. https://doi.org/10.1038/s41588-018-0333-3.
48. Wulff, K., Gatti, S., Wettstein, J.G., and Foster, R.G. (2010). Sleep and circadian rhythm disruption in psychiatric and neurodegenerative disease. Nat. Rev. Neurosci. *11*, 589–599. https://doi.org/10.1038/nrn2868.
49. Nutt, D., Wilson, S., and Paterson, L. (2008). Sleep disorders as core symptoms of depression. Dialogues Clin. Neurosci. *10*, 329–336. https://doi.org/10.31887/DCNS.2008.10.3/dnutt.
50. Wang, C., and Holtzman, D.M. (2020). Bidirectional relationship between sleep and Alzheimer's disease: role of amyloid, tau, and other factors. Neuropsychopharmacology *45*, 104–120. https://doi.org/10.1038/s41386-019-0478-5.
51. Kalia, L.V., and Lang, A.E. (2015). Parkinson's disease. Lancet *386*, 896–912. https://doi.org/10.1016/S0140-6736(14)61393-3.
52. Ferrarelli, F., Huber, R., Peterson, M.J., Massimini, M., Murphy, M., Riedner, B.A., Watson, A., Bria, P., and Tononi, G. (2007). Reduced sleep spindle activity in schizophrenia patients. Am. J. Psychiatry *164*, 483–492. https://doi.org/10.1176/ajp.2007.164.3.483.
53. Ferrarelli, F., and Tononi, G. (2016). What Are Sleep Spindle Deficits Telling Us About Schizophrenia? Biol. Psychiatry *80*, 577–578. https://doi.org/10.1016/j.biopsych.2016.08.012.
54. Mariani, S., Tarokh, L., Djonlagic, I., Cade, B.E., Morrical, M.G., Yaffe, K., Stone, K.L., Loparo, K.A., Purcell, S.M., Redline, S., and Aeschbach, D. (2018). Evaluation of an automated pipeline for large-scale EEG spectral analysis: the National Sleep Research Resource. Sleep Med. *47*, 126–136. https://doi.org/10.1016/j.sleep.2017.11.1128.
55. Uhlhaas, P.J., and Singer, W. (2013). High-frequency oscillations and the neurobiology of schizophrenia. Dialogues Clin. Neurosci. *15*, 301–313. https://doi.org/10.31887/DCNS.2013.15.3/puhlhaas.
56. Oostenveld, R., Fries, P., Maris, E., and Schoffelen, J.M. (2011). FieldTrip: Open source software for advanced analysis of MEG, EEG, and invasive electrophysiological data. Comput. Intell. Neurosci. *2011*, 156869. https://doi.org/10.1155/2011/156869.
57. Staresina, B.P., Bergmann, T.O., Bonnefond, M., van der Meij, R., Jensen, O., Deuker, L., Elger, C.E., Axmacher, N., and Fell, J. (2015). Hierarchical nesting of slow oscillations, spindles and ripples in the human hippocampus during sleep. Nat. Neurosci. *18*, 1679–1686. https://doi.org/10.1038/nn.4119.
58. Can, A., Dao, D.T., Terrillion, C.E., Piantadosi, S.C., Bhat, S., and Gould, T.D. (2012). The tail suspension test. J. Vis. Exp. *59*, e3769. https://doi.org/10.3791/3769.

STAR★METHODS

KEY RESOURCES TABLE

REAGENT or RESOURCE	SOURCE	IDENTIFIER
Chemicals, peptides, and recombinant proteins		
Melatonin	NATURE'S BOUNTY	N/A
Zoletil 50	Virbac S.A.	N/A
Meloxicam	Qilu Animal Health Products Co., Ltd.	150252467
Aripiprazole	MedChemExpress	HY-14546
Experimental models: Organisms/strains		
Wild type (WT) cynomolgus monkeys	Songjiang Non-human Primate Facility of Institute of Neuroscience	N/A
BMAL1-ablated cynomolgus monkeys	Songjiang Non-human Primate Facility of Institute of Neuroscience	N/A
C57BL/6J mice	Shanghai Lingchang Biotechnology Co., Ltd.	N/A
Bmal1-floxed mice	Jackson Laboratory	JAX007668
Ella-cre mice	Jackson Laboratory	JAX003724
Software and algorithms		
NeuroScore v3.2.1x Core Software	Data Sciences international	271-0165-320
Ponemah-6	Data Sciences international	PNM-P3P-CFG
Matlab	MathWorks	N/A
FieldTrip	fieldtriptoolbox.org	N/A
GraphPad Prism 9	GraphPad	N/A
Other		
PhysioTel HD implants	Data Sciences international	HD-X02
PhysioTel Implant	Data Sciences international	L03

RESOURCE AVAILABILITY

Lead contact

Further information and requests for resources should be directed to and will be fulfilled by the lead contact, Hung-Chun Chang (hcchang@lglab.ac.cn).

Materials availability

This study did not generate new unique reagents.

Data and code availability

- Data reported in this paper will be shared by the lead contact upon request.
- This paper does not report original code.
- Any additional information required to reanalyze the data reported in this paper is available from the lead contact upon request.

EXPERIMENTAL MODEL AND STUDY PARTICIPANT DETAILS

Cynomolgus monkey and mouse

Five cynomolgus monkeys (*Macaca fascicularis*), including a female and two male BMAL1-ablated monkeys,[14] and age-matched wild-type monkeys (one female and two male) were used in this study. The electroencephalography and locomotive activity were recorded at near 5 years of age. C57BL/6J male mice at different ages (2 - 14 months old) were used in this study. The *Bmal1*-floxed strain was obtained from the Jackson Laboratory (JAX007668), then bred with *Ella*-cre (JAX003724) to achieve whole body heterozygous Bmal1-deletion. The heterozygous *Bmal1*-deleted mouse line was then back-crossed to C57BL/6J for five generations prior to the standard heterozygote x heterozygote breeding for whole body *Bmal1*-knockout mice. All animals were housed in a conditioned environment (temperature: 22 ± 1°C; humidity: 50% ± 5%) with a 12-h L/D cycle (light-on time 07:00 to 19:00). The use and care of cynomolgus monkeys and mice were complied with

the ethical guidelines of the Institute of Neuroscience, Shanghai Institutes for Biological Science, Chinese Academy of Science (ION-2019043 and ER-SIBS-221106P) and Lingang laboratory.

METHOD DETAILS

Electroencephalography recording

Monkey EEG recording was carried out by implanting radio telemetry transmitters (PhysioTel Digital L03 implant, Data Sciences International (DSI)) for monitoring continuous long-term locomotive activity, body temperature and biopotential signals including electromyography (EMG). Monkeys were deeply anesthetized by single intramuscular dosing of 5 mg/kg Zoletil 50 (Virbac S.A.) before implantation surgery. An additional dosing of 1 mg/kg Zoletil 50 was provided intramuscularly to maintain deep anesthetization if the surgery exceeded 4 hours. The DSI implant was subcutaneously embedded at the waist. The EEG electrode biopotential leads were tunneled subcutaneously to the skull, and the EEG electrodes were screwed into the skull near Fz position for EEG signal sampling.[39,54,55] Electrode leads for EMG were sutured to the neck musculature. After surgery, monkeys were provided with daily analgesia Meloxicam (1 mg/kg) intramuscularly for 3 days, and daily antibiotics (Penicillin, 20 MU/kg) for one week in their home cages. The housing area for EEG/EMG recording (8.9×2.5×2.8 m) was equipped with nine transceivers (TRX-1) mounted to the walls, ensuring excellent sampling of telemetric signals covering the entire room. The TRX-1 transceivers were connected to a data-exchange matrix (CLC) then to a computer for recording and data storage. After recovery from surgery, biopotential signals were monitored under three different conditions for monkeys: normal light-dark cycle (12-hr light and 12-hr dark, L/D) for two days, 24-hr light exposure (L/L) for two days, and melatonin treated under L/L for two days. Melatonin (2 mg/kg, Nature Made, USA) were fed each day at 19:00. Similar procedures were applied for mouse recording with the used of HD-X02 implant (DSI). The two EEG electrodes were screwed into the skull 1 mm lateral, and 1 or 3 mm anterior to the Bregma, respectively. Activity, body temperature, EEG and EMG signals were collected by the RPC-1 receiver connected to a MX2 hub and a computer. The recordings were carried out under three housing conditions: normal light-dark cycle (12-hr light and 12-hr dark, L/D) for two days, constant dark (D/D) for two days, and constant illumination (L/L) for two days. Software NeuroScore 3.2.1 (DSI) was applied for primary sleep analysis of monkey and mouse EEG to identify awake, REM and NREM sleep stages. Briefly, 10-second epochs with high delta power, low beta power, low EMG activity and without locomotion were classified as NREM sleep; epochs with high theta power, low beta power, low EMG activity and without locomotion were classified as REM sleep; and the rest epochs were classified as awake states. For monkey EEG, the primary NREM/REM/awake states were staged with same standards as for mouse EEG. The NREM epochs were further separated into slow wave sleep (SWS) and N1/N2 stages according to the clustering result and distribution of the delta oscillation amplitudes.

EEG data processing, filtering, and artifact rejection

All the EEG data were filtered with three-order Butterwoth's filter (Matlab). The classical frequency bands used in the analysis of monkey EEG are as following: dc wave, [0, 0.5] Hz; delta wave: [0.5, 4] Hz; theta wave: [4, 8] Hz; alpha wave: [8, 12] Hz; beta wave: [13, 32] Hz; gamma wave [32, 100] Hz. The toolboxes of FieldTrip[56] and DSI Ponemah-6 (Data Sciences International) were applied to view EEG and body temperature data. Analysis was performed with Matlab (MathWorks). The rejection of artifacts and possible seizures were identified according to an established method[57] that marked conjunction of amplitude z-score exceeded 3 as artifacts.

Kullback–Leibler divergence

The Kullback–Leibler divergence (KLD, relative entropy) was applied to measure the difference of one probability distribution from another-reference probability distribution, in the current study, for the comparison of night versus day EEG. After filtered with Butterworth filter, energy of each 10-s epoch of each EEG band was calculated. The resulting epoch powers were classified into night-day pair sections, followed by calculating the respective probability distributions. The Kullback–Leibler divergence was calculated with the following formula:

$$KL(P_{f,s2} \| Q_{f,s1}) = \sum_i Q_{f,s1}(i) ln \frac{Q_{f,s1}(i)}{P_{f,s2}(i)}$$

Q presents the distribution of the absolute EEG activity at a particular band f under state s1 during light-on, P indicates the distribution of EEG activity at same frequency band f, in the other state s2 during light-off.

Behavioral recordings in novel environment

To study the behavioral and physiological responses to the change of environment, monkeys were released into a novel cage (1.75*0.95*1.3 m) for free exploration for 10 minutes, then another 5-minute stroll with the experimenter presence. Behavioral responses/movement and EEG data were collected via video recording and telemetry device (DSI). Behavioral responses were classified into normal or abnormal (self-injuring, curl-up, or delusion-like) status, then correlated to EEG power every 10 seconds. The three abnormal phenotypes proposed in the study were unique to BKO monkeys and did not occur in WT monkeys during experiments. Briefly, self-injuring included self-biting and self-beating events. Curling-up behavior was scored by lying aside with one shoulder or one side of the body touching the ground. Delusion-like behaviors included events such as raising fist in the air and gazing at the surroundings slowly but sitting still. EEG signals were filtered with Butterwoth's filter as described and then calculated for EEG power with every 2 Hz band window. Antipsychotic Aripiprazole (0.1mg/kg)

was intravenously administrated for the female BMAL1-ablated monkey, then recorded for a 15-minute novel cage exploring 2 hours post drug treatment.

Behavioral recordings in mice

To study stress responses in Bmal1-KO mice, the tail suspension test and the open field test were applied for the inspections. For tail suspension test, 8-month-old Bmal1-KO mice (n=3) were tail-adhered and suspended individually for an approximate distance of 20 cm from the mouse nose to the apparatus floor[58] for 6 minutes of EEG and video recordings. Mobile events and immobile events were scored, and the corresponding EEG data were extracted (DSI) and analyzed. For the open field test, Bmal1-KO mice were placed in a 30*30 cm cage individually for EEG and video recordings for 15 minutes. The moments of mouse travel in the inner zone (15*15 cm area in the cage center) and outer zone were marked for EEG data correlation. Events were marked for EEG data extraction and analysis (DSI). EEG signals were filtered with Butterwoth's filter, and then calculated for EEG power with every 2 Hz band window.

QUANTIFICATION AND STATISTICAL ANALYSIS

Data were represented as mean ± SEM. Two-way ANOVA with Bonferroni correction for multiple comparisons was performed in Figures 2D, 3D, 5A–5E, 6B, S3A, S3B, S4B, and S4C, and the p values between indicated groups were shown within panels. Unpaired two-tailed Student's t-test was performed in Figures 1A–1D, 6D, 6F, S5, S6A, S8A, and S9A, and statistical significances are labelled on top as ns not significant; *$p < 0.05$; **$p < 0.01$; ***$p < 0.001$. AUC (Area Under the ROC Curve) was performed in Figure S7. All statistical analyses are calculated using GraphPad Prism software (Prism version 9.0).